Journal of Medicinal Chemistry

Article

The design, synthesis and evaluation of triazole derivatives that induce Nrf2 dependent gene products and inhibit the Keap1-Nrf2 protein-protein interaction

Hélène Bertrand, Marjolein Schaap, Liam Baird, Nikolaos D. Georgakopoulos, Adrian Fowkes, Clarisse Thiollier, Hiroko Kachi, Albena T. Dinkova-Kostova, and Geoffrey Wells

J. Med. Chem., **Just Accepted Manuscript** • DOI: 10.1021/acs.jmedchem.5b00602 • Publication Date (Web): 08 Sep 2015

The design, synthesis and evaluation of triazole derivatives that induce Nrf2 dependent gene products and inhibit the Keap1-Nrf2 protein-protein interaction

*Hélène C. Bertrand[1,†], Marjolein Schaap[1], Liam Baird[2,††], Nikolaos D. Georgakopoulos, Adrian Fowkes[1], Clarisse Thiollier[1], Hiroko Kachi[1], Albena T. Dinkova-Kostova[2,3], Geoff Wells[1,]**

[1]UCL School of Pharmacy, University College London, 29/39 Brunswick Square, London, WC1N 1AX, United Kingdom

[2]Jacqui Wood Cancer Centre, Division of Cancer Research, Medical Research Institute, University of Dundee, Dundee, Scotland, United Kingdom

[3]Departments of Medicine and Pharmacology and Molecular Sciences, Johns Hopkins University School of Medicine, Baltimore, MD, USA

KEYWORDS: Keap1, NQO1, Nrf2, protein-protein interactions

ABSTRACT: The transcription factor Nrf2 regulates the expression of a large network of cytoprotective and metabolic enzymes and proteins. Compounds that directly and reversibly inhibit the interaction between Nrf2 and its main negative regulator Keap1 are potential pharmacological agents for a range of disease types including neurodegenerative conditions and cancer. We describe the development of a series of 1,4-diphenyl-1,2,3-triazole compounds that inhibit the Nrf2-Keap1 protein-protein interaction (PPI) *in vitro* and in live cells and up-regulate the expression of Nrf2-dependent gene products.

Introduction Sustained oxidative stress and inflammation have been proposed as crucial steps in the aetiology of chronic neurodegenerative conditions and cancer. A promising strategy to mitigate these effects and curtail the development of these conditions involves inducing the expression of cytoprotective proteins under the control of the transcription factor nuclear factor erythroid 2 p45-related factor 2 (Nrf2). Nrf2 is a cap 'n' collar basic leucine zipper transcription factor that regulates the expression of genes with antioxidant response element (ARE) sequences in their promoter regions. The genes controlled by Nrf2 encode a group of around 500 proteins that have roles in metabolism (*e.g.* NAD(P)H quinone oxidoreductase-1 (NQO1), heme oxygenase-1 (HO1), glutathione conjugation enzymes), redox homeostasis (*e.g.* glutathione biosynthetic and reducing enzymes, thioredoxin, thioredoxin reductase) and autophagy (*e.g.* sequestosome-1/p62) amongst other processes.[1-3] In particular, up-regulation of phase II drug metabolism enzymes plays a role in removing the polar, reactive products of primary (phase I) metabolites, thereby limiting their genotoxic potential.

There has been considerable progress recently in understanding the regulation of Nrf2 in the cellular context and this has provided a number of intervention opportunities to control its activity. The activity of Nrf2 under basal conditions is limited by its short half-life (< 10 min).[4, 5] This is controlled largely by the rapid ubiquitination and proteosomal destruction of Nrf2, a process that is orchestrated by the ubiquitination facilitator protein Kelch-like ECH-associated protein 1 (Keap1).[6-9] A 'hinge and latch' mechanism has been proposed in which two sites in the Nrf2 *N*-terminal Neh2 domain interact with Keap1, a high affinity ^{79}ETGE^{82} 'hinge' motif (Kd ~ 5 nM) that tethers Nrf2 to one arm of the Keap1 dimer and a lower affinity ^{26}QDIDLG^{31} 'latch' motif (Kd ~ 1000 nM).[10] Keap1 uses a cyclical mechanism to target Nrf2 for degradation, whereby Nrf2 binds sequentially to the Keap1 dimer, first through the high affinity motif to form the open conformation of the Keap1-Nrf2 protein complex, and then through the lower affinity motif to form the closed conformation of the complex.[11] The closed conformation allows ubiquitination of lysine residues in the intervening Neh2 domain sequence of Nrf2 via a pendant Cullin 3 ubiquitination complex.[12-15] The ubiquitinated Nrf2 is released from Keap1 and degraded by the 26S proteasome, free Keap1 is regenerated and able to bind to newly translated Nrf2, and the cycle of Keap1-mediated degradation of Nrf2 begins again.

Under conditions of oxidative stress, or on exposure to electrophilic compounds, cysteine sensors within Keap1 (e.g. Cys151, 273, 288) are oxidized or conjugated, leading to accumulation of the closed conformation of the Keap1-Nrf2 complex. It is proposed that the resulting structural change inactivates the ubiquitination process, Nrf2 is not released, and free Keap1 is not regenerated, allowing newly synthesized Nrf2 to accumulate within the cell and exert its transcriptional activity.[1, 16-18] A number of electrophilic Nrf2 inducers have been widely studied, including the broccoli-derived isothiocyanate compound sulforaphane **1** and the

synthetic compound oltipraz **2** (Figure 1).[1, 16-19] Sulforaphane up-regulates the expression of a range of ARE-responsive genes in treated cells and has cytoprotective effects *in vivo* including reducing the number of tumors that develop in carcinogen exposure studies.[20, 21] Furthermore, in humans, intervention with sulforaphane-rich broccoli sprouts accelerates the detoxification of aflatoxin and airborne pollutants, suggesting frugal means to counteract the health risk associated with long-term exposures of environmental toxins.[22, 23] Sulforaphane also has promise for treatment of autism spectrum disorder – a recent placebo-controlled, double-blind, randomized clinical trial has shown that young men with autism who received daily oral doses of broccoli sprouts delivering sulforaphane (50-150 μmol) for 18 weeks had significant improvement in social interaction, abnormal behavior, and verbal communication.[24]

An alternative approach to enhance Nrf2 activity involves direct disruption of the Keap1-Nrf2 interaction at the protein-protein interface. Thus compounds that interact with the Keap1 Kelch domain have the potential to disrupt Nrf2 binding in a reversible manner and inhibit its ubiquitination. Such compounds may have advantages over electrophilic inducers that include improved specificity and reduced off-target effects due to the lack of a covalent interaction. We and others showed that peptides (*e.g.* **3**-**5**) that mimic Nrf2 were able to disrupt the Keap1-Nrf2 interaction.[25-29] A few small molecule Nrf2 activators that inhibit the Keap1-Nrf2 protein-protein interaction (PPI) have been reported recently, confirming the potential of a direct targeting strategy. These direct small molecules inhibitors were identified by virtual screening (**6**, **7**), high throughput screening (**8**-**10**) and subsequent SAR studies, or by structure-based design and molecular determinants analysis (**11**) (Figure 1).[30-35]

In this study we have used the available crystal structures of the human Keap1 Kelch domain, both alone[36] and in complex[14] with peptides to identify potential small molecule inhibitors of the

Keap1-Nrf2 protein-protein interaction using an *in silico* fragment-based approach. Analysis of the binding poses and protein-interactions of the most recurrent molecular scaffolds led us to propose the 1,4-diaryl-1,2,3-triazole scaffold as a candidate for SAR investigations. As docking of a prototypical ligand of this new series demonstrated encouraging scores, we synthesized small libraries of 1,4-diaryl-1,2,3-triazoles and evaluated their ability to disrupt the Keap1-Nrf2 PPI using a fluorescence polarization assay that we developed and validated previously.[25] In parallel, we investigated their ability to induce the expression of the Nrf2 target enzyme NQO1 in Hepa1c1c7 cells, an assay that has been widely applied in the discovery and evaluation of Nrf2 inducing agents.[37, 38] Further studies in dose response experiments allowed us to extract favorable features for biological activity and to identify a narrow set of compounds with promising activity. Compound **22s** was not cytotoxic over a wide concentration range, showed up-regulation of Nrf2 protein levels and induced the expression of downstream gene products in a manner comparable to that of sulforaphane **1**. Intriguingly, **22s** appears to disrupt the PPI in live cells in a manner that is distinct from sulforaphane and other electrophilic inducers. Recently we have shown that compound **22s** (PMI, HB229) is a promising tool compound in the area of mitochondrial autophagy (mitophagy).[39] It appears to induce mitophagy in a p62 and Nrf2 dependent manner, but its activity is only partially dependent upon Parkin and PINK1. In this respect the compound has intriguing functional differences from the prototype inducers of mitophagy, the ionophores CCP and FCCP, and from **1** which lacks equivalent mitophagy-inducing activity.

Compound Design Compounds from a subset of the ZINC database ("clean fragments", ~178,000 compounds)[40] were docked into the human Keap1 C-terminal Kelch domain structure (PDB entry: 2FLU) in the Nrf2 'ETGE' peptide binding site[14] and ranked using the Autodock 4.2

and DOCK 6.6 software packages.[41, 42] After further refinement of the highest scoring ligands (Autodock $\Delta G_{binding} \leq$ -7.5 kcal/mol) using extended docking protocols, the 364 highest-scoring molecules (Autodock $\Delta G_{binding} \leq$ -8.0 kcal/mol) were selected and analyzed. The results indicated that a relatively small group of molecular scaffolds dominated the compound set; common features could be identified in these recurrent scaffolds and in hits recently identified by structure-based virtual screening.[31] Two examples, compounds **12** and **13**, are shown in Figure 2. Although compound **12** contains a thiazolidinone moiety, a known PAINS (Pan-Assay Interference Compounds)[43] substructure, it was included in our initial analyses because related 2-oxo-rhodanine derivatives have been shown to interact reversibly with Keap1 in fluorescence anisotropy assays (the authors did not present data regarding cell-based activity).[31] However, we did not pursue SAR studies with **12** beyond the *in silico* evaluation. Analysis of the calculated binding modes of the highest-scoring compounds suggested that carboxylate or nitro substituents formed favorable electrostatic and hydrogen bond interactions with the Arg 380, 415, 483 and Asn 382 residues of Keap1, in some cases the scaffold formed additional hydrogen bond interactions with, for example, the side chain of Ser 602 within the binding site (Figure 2). Using the distances between the favorable substituent features of the highest-scoring docked ligands and the distance between the glutamate side chains of the Nrf2 ETGE sequence as a guide, we designed a new series of ligands based upon a simple 1,4-diaryl-1,2,3-triazole scaffold that can be both easily synthesized and functionalized to mimic the pharmacophores identified from the docking exercise. Our initial docking studies with compounds from this series suggested that the calculated binding energies should be similar to those identified by virtual screening and that they could form similar interactions within the binding pocket (Figure 2, e.g. **24d**).

Synthesis and Fixed-Dose Screening We initially synthesized a small combinatorial library of 36 1,4-diaryl-1,2,3-triazoles by reacting ethynyl- and azido-benzene intermediates bearing *meta* or *para* nitro, carboxylic acid or carboxamide groups (**21-26a-f**, Scheme 1). The compounds were synthesized by copper catalyzed alkyne-azide cycloadditions under microwave irradiation (Scheme 1). The azidobenzene intermediates **14** were prepared using standard azidation conditions from the corresponding anilines or by direct substitution of a halogen-substituted benzene (using NaN_3 in DMF). The ethynylbenzene precursors **15-20** were prepared in two steps from the corresponding halogenated derivatives by Sonogashira coupling with trimethylsilylacetylene followed by cleavage of the TMS group by treatment with K_2CO_3 in MeOH.

The compounds were screened *in vitro* using a fluorescence polarization assay that we developed previously in which we evaluated the ability of **21-26a-f** to disrupt the interaction between the Kelch domain of Keap1 and a fluorescein labelled peptide based on the high affinity 'ETGE' motif from Nrf2 (FITC-β-DEETGEF-OH, β for β-alanine).[25] We have demonstrated that the native Nrf2 Neh2 domain is capable of displacing the fluorescent peptide with a K_i of ~ 25 nM, consistent with the K_d determined using isothermal calorimetry of 5.3 nM.[25] The competition experiment was initially carried out using a fixed 100 μM concentration of inhibitor (**21-26a-f**, Table 1). Five of the six compounds with a *meta*-carboxylic acid substituent on the triazole 4-phenyl ring exhibited encouraging activity (**24a**,**c-f**). Compounds bearing a 4-carboxamide substituent in the 4-phenyl ring (**25a-e**) appeared to interfere consistently with the FP signal (FP value greater than the control), despite the molecules lacking innate fluorescence properties. However, otherwise there was not a significant discrimination between the *meta* or *para* substitution pattern on either the 1- (R^1) or 4-phenyl (R^2) substituent.

In addition to the fixed dose FP assays we screened the 36-member library to evaluate Nrf2 dependent transcription using an established colorimetric NQO1 induction assay in Hepa1c1c7 mouse hepatoma cells.[37, 38] Initially we tested the compounds at a fixed concentration of 10 μM, with an exposure time of 24 h (Table 1). Results from the NQO1 induction experiments were more discriminating than the fixed dose FP assay; six compounds induced NQO1 expression > 1.5-fold. Of these compounds four had a 4-(3-nitrophenyl)triazole motif (**22**, Scheme 1). All of the active compounds had a nitro/nitro or nitro/carboxamide substitution pattern. In contrast many of the compounds with carboxylic acid substituents were inactive (relative induction ~1). The lack of activity of the carboxylate derivatives may relate to poorer cell penetration due to their net negative charge at physiological pH. Based upon the observations from the fixed dose FP and NQO1 assays, including the relatively good activity in the FP assay, combined with promising cell-based activity (Table 1) we chose a *meta*-nitro substitution on the 4-phenyltriazole moiety for the second generation library.

The second series (**22g-t**) was synthesized using 1-ethynyl-3-nitrobenzene **16** and an array of azidobenzenes **14g-t** bearing substituents in the 3-position with a range of electronic and steric properties (Scheme 2). Compounds **22g-t** showed consistent activity in the FP assay with percentage inhibitions in the 60-80% range (100 μM fixed dose) with the exception of compounds **22p** (R^1 = F) and **22t** (R^1 = CN), which were less active. All of the compounds showed promising activity in the NQO1 induction assay with compound **22s** (R^1 = I)[39] demonstrating a robust 4-fold induction at 10 μM (Table 2).

As the carboxylic acid function appeared to confer favorable activity in the FP assays, but was detrimental in the cell-based NQO1 assays, we prepared a third series of compounds to examine the influence of a tetrazole moiety as a carboxylate isostere. We first envisioned the synthesis of

tetrazoles from the corresponding carboxamide compounds synthesized in the first library, using $SiCl_4$ and NaN_3 in a mixture MeCN/DMF.[44] No reaction occurred in these conditions, which led us to consider the synthesis of the tetrazole ring from a cyano precursor. Using 1-ethynyl-3-cyanobenzene **27** and a small series of 3-substituted-phenylazides selected from the previous screening exercise (**14b**,**c**,**h**,**l**,**q**,**s**,**t**), a series of 1,2,3-triazoles **28** was prepared. This series was evaluated along with the corresponding tetrazoles **29** that were synthesized in good yields by [3+2] cycloaddition of the cyano compounds with NaN_3 in a sealed tube, using ammonium chloride and catalytic lithium chloride in refluxing DMF (Scheme 3, Table 3).[45]

The tetrazoles and their cyano precursors were tested in the fixed dose FP assay at a concentration of 100 μM (Table 3); only two of the compounds showed significant activity, **29b** and **29c** (~70% inhibition). The EC_{50}s of these two tetrazolo-compounds, determined in a dose-response experiment (*vide infra*), were >50 μM. The NQO1 induction ability (Table 3) was generally poor indicating that they were not effective Nrf2 inducers and that in this context the tetrazole substituents were relatively poor carboxylate isosteres.

Dose-Response Evaluation of Selected Analogues Based upon the fixed dose assessments, a selection of compounds from the **22a-t** series was tested in FP and NQO1 dose response assays. The EC_{50}s of compounds were in the range 5-39 μM (Table 4). Compounds **22d** ($R^1 = CO_2H$), **22h** (R^1 = Me), **22q** (R^1 = Cl) and **22s** (R^1 = I) were the most active with EC_{50} values in the range 5-10 μM. A further five compounds displayed intermediate activity with EC_{50} values in the 11-15 μM range: **22b** ($R^1 = NO_2$), **22l** (R^1 = OEt), **22o** ($R^1 = NMe_2$), **22k** (R^1 = OMe), **22m** (R^1 = 1,3-dioxolane). The results indicate that a range of substituents is tolerated at this position, with the possible exception of the t-butyl (**22i**, 37.8 μM) and thiomethyl (**22n**, 38.5 μM) substituents. Compound **22s** was evaluated further in the FP assay. Experiments in the presence of varying

concentrations of the detergent Triton X100 (0 – 1% v/v) showed no change in the EC_{50} of the compound (Figure S2). Treatment of the Keap1 protein with **22s** for 2.5 h followed by dialysis yielded protein that demonstrated a similar Kd to Keap1 treated with buffer alone (Figure S3). Taken together these data provide support for the proposed reversible binding of **22s** to Keap1.

The *in vitro* activity of the most active compounds determined in the dose-response competitive FP assay is close to the inhibitory potency of peptides described previously that mimic the 'ETGE' and the 'DLG' motifs (**3** and **5**, EC_{50} = 5.4 μM and 17.1 μM respectively, Figure 3).[25] In the 'hinge and latch' type binding mechanism suggested for the interaction of Nrf2 with Keap1, both motifs must be bound to allow ubiquitination of Nrf2.[11, 17] In principle, disruption of the interaction of the low affinity 'DLG' motif alone would thus be sufficient to prevent the ubiquitination of Nrf2 and allow its release from Keap1 tethering.

The same group of compounds was evaluated along with the prototype Nrf2 inducing agents sulforaphane **1** and oltipraz **2** (positive controls) in a dose response assay to determine the concentration range over which NQO1 induction occurred.[37, 38] The results (Table 4) are expressed as the concentration required to induce a two-fold increase in NQO1 enzymatic activity (CD value) after 24 h. Five compounds exhibited CD values below 1.5 μM, indicating activities that are comparable to **1** (0.25 μM) and **2** (10.2 μM). There is a relatively good correlation between the FP assay EC_{50} concentrations and the NQO1 assay CD values with compounds **22h**, **22q** and **22s** showing promising activity in both experiments.

Stabilization of Nrf2 and induction of Nrf2-dependent genes We selected three compounds with differing activity in the FP and NQO1 assays for further evaluation (**22h**, **22i** and **22s**). Compound **22i** was less active in the FP assay and did not significantly induce NQO1 enzymatic

activity, whereas **22h** and **22s** showed similar activity in the FP experiments and induction of NQO1 in the low micromolar range (Table 4, Figure 3). The effects of the compounds on Nrf2 activity were evaluated in Hepa1c1c7 cells and compared with sulforaphane **1** (Figure 3). The cells were incubated with the compounds at a fixed concentration of 10 μM with different exposure times. Treatment with **1**, **22h** and **22s** resulted in a marked increase in Nrf2 protein levels (Figure 3), comparable after 6 h to those produced by **1**; the effect from **22i** was reduced compared to the other compounds. The increase in Nrf2 levels was time-dependent; the highest level of induction occurred after 3-6 h for **22s** whereas for **1**, maximal induction was achieved after 1 h. Up-regulation of the expression of the Nrf2-dependent enzymes HO-1 and NQO1 was also observed. For these proteins, the time course was the same for both **22h**, **22s** and **1**; peak HO-1 induction occurred after 6 h, but NQO1 protein was not detected before 24 h, consistent with previously reported differences in kinetics of their transcripts.[46] The effect of **22i** on HO-1 expression was significant although up-regulation of NQO1 was close to undetectable. This suggests that the compounds may have differential effects on downstream targets, an observation that warrants further investigation.

Disruption of the Keap1-Nrf2 interaction in live cells As **22s** was the most robust inducer in these series, we next evaluated the ability of this compound to disrupt the Keap1-Nrf2 interaction in live cells by use of a FRET-based assay system in which Keap1 was labelled with the fluorophore mCherry and Nrf2 was labelled with EGFP, as previously described.[11, 47] These proteins when ectopically expressed into HEK293 cells recapitulate the native Keap1-Nrf2 interaction.[11] Fluorescence lifetime imaging microscopy (FLIM) was then used to determine the timescale over which EGFP fluorescence emission occurs. Shorter lifetimes reflect a more efficient energy transfer to the mCherry FRET partner, whereas longer timescales reflect

dissociation of the complex. The distribution of FRET efficiencies (FE) associated with individual pixels in the microscopy images is related to the proximity of the two fluorophores. Previous experiments have characterized two FE populations, a low (~13%) FE population in which the fluorophores are relatively distant from each other, corresponding to Nrf2 bound to Keap1 by only the high affinity ETGE motif (termed 'open' conformation of the Keap1-Nrf2 complex), and a high (~21%) FE population in which the fluorophores are closer together, in which Nrf2 is bound to Keap1 by both the low affinity DLG and high affinity ETGE motifs (termed 'closed' conformation of the Keap1-Nrf2 complex).[11]

Exposure to electrophilic inducers such as sulforaphane **1**, causes accumulation of the complex in the 'closed' conformation, and it was proposed that, in this electrophile-inactivated 'closed' complex, Nrf2 is not ubiquitinated or released by Keap1, which means that the free Keap1 dimer is not regenerated, allowing newly synthesized Nrf2 to accumulate.[11] In contrast to sulforaphane **1** and other electrophilic inducers, when **22s** (10 μM) was administered to HEK293 cells that had been co-transfected with EGFP-Nrf2 and Keap1-mCherry, the high FE population was diminished and the low FE population predominated (Figure 4 and Tables S1, S2). This suggests that the compound disrupts the interaction between the Nrf2 DLG motif and Keap1, but not the ETGE motif. This observation is consistent with direct inhibition of the Keap1-Nrf2 protein-protein interaction.

Cytotoxicity We then compared the cytotoxicity of **22s** and **1** in Hepa1c1c7 cells using a sulforhodamine B cytotoxicity assay. **22s** was not cytotoxic (cell viability ~100%) up to a concentration of 200 μM over 24 and 48 h periods. **1** exhibited cytotoxicity at a concentration greater than 10-30 μM, indicating that **22s** has a broader therapeutic window for NQO1

induction (Figure S1). For **1** the therapeutic (chemopreventive) index ([cytotoxicity GI_{50}]/[NQO1 CD]) was ~250 in the Hepa1c1c7 cell line, compared to that of **22s** which was >1000.

Conclusion In this study we developed a series of compounds with a 1,4-diaryl-1,2,3-triazole scaffold using input from virtual screening of a fragment library combined with structural and distances considerations. We have synthesized three small libraries of triazole derivatives bearing a range of substituents on the 1- and 4-aryl substituents. Amongst the substitution patterns evaluated the best combinations for cell-based activity were a *meta*-nitro group on the 4-phenyl ring and a *meta*-nitro, methyl or halogen on the 1-phenyl unit. The ability of three compounds **22h**, **22i** and **22s** to stabilize Nrf2 and induce the expression of its target genes NQO1 and HO-1 in a concentration- and time-dependent manner correlated with the activity of the compounds in the PPI FP assay. The most active compound **22s** binds reversibly to Keap1 and was not cytotoxic over a wide concentration range, but had similar cell-based activity to sulforaphane **1**. Intriguingly, live cell-based imaging experiments suggest that **22s** drives the formation of the 'open' conformation of the Keap1-Nrf2 complex. Overall, the molecular modeling and experimental results are consistent with direct targeting of the Keap1-Nrf2 interaction. Further detailed investigations are underway to elucidate the precise underlying mode of action. Despite the structural simplicity of this compound, it has intriguing properties as both a cell permeable biochemical probe for Nrf2 activation and mitophagy,[39] and as a template for further structural refinement.

FIGURES

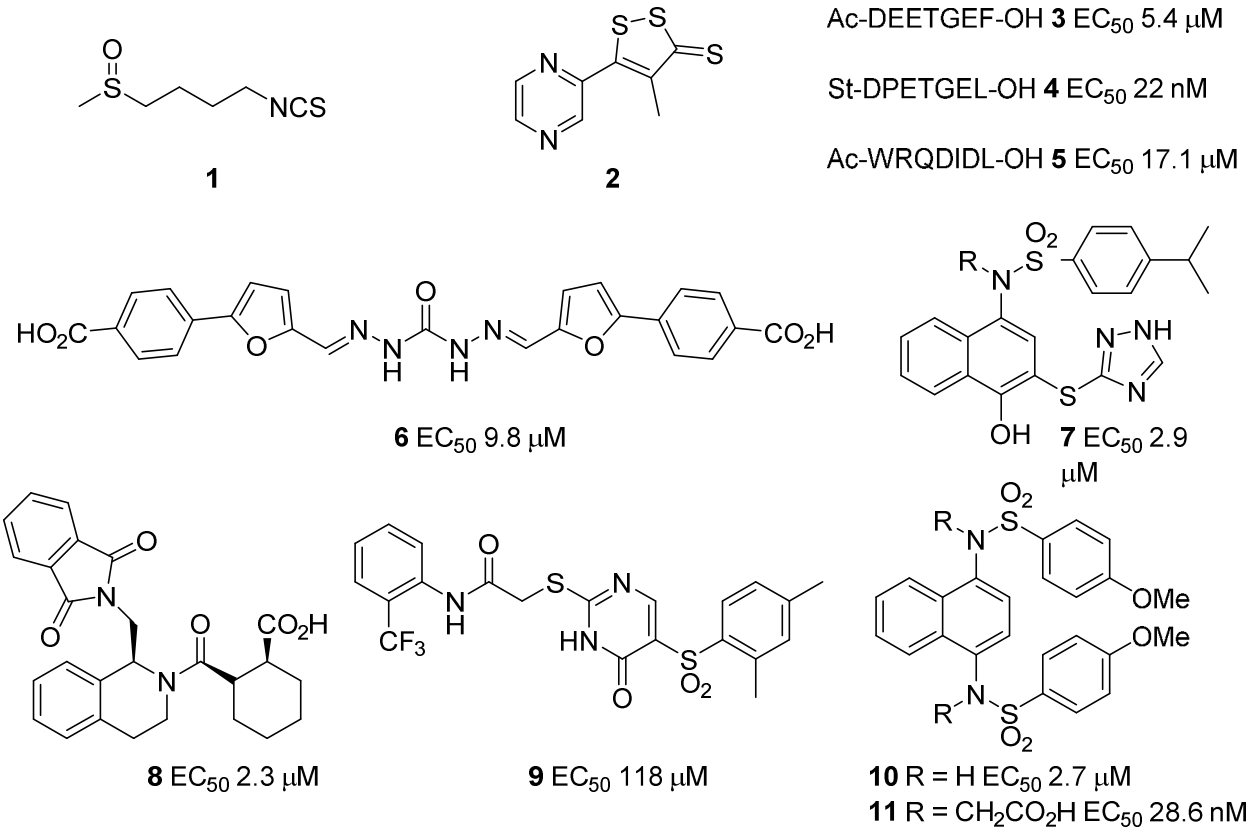

Figure 1. Structures of known indirect (e.g. **1**, **2**) and direct (**3-11**) Keap1-Nrf2 inhibitors with their EC_{50} values for inhibition of the Keap1-Nrf2 interaction.[30-35]

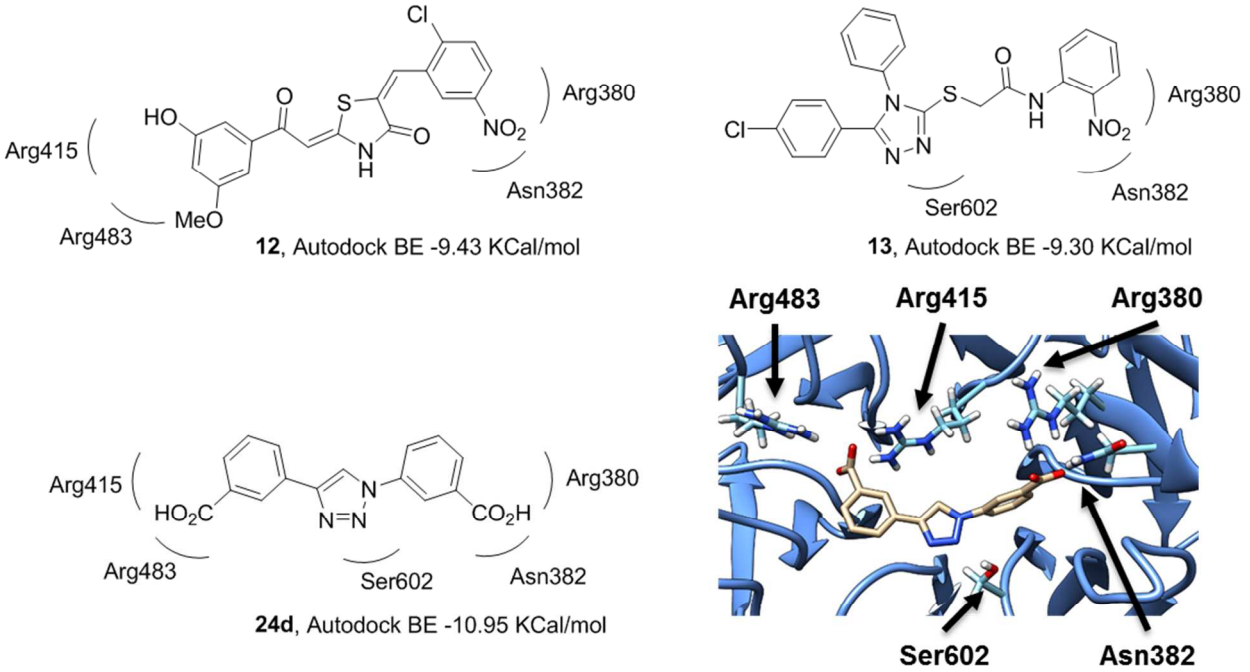

Figure 2. Scaffolds **12** and **13** identified using *in silico* docking calculations (top) and the diaryl triazole scaffold (e.g. **24d**) docked in the Keap1 Kelch domain.

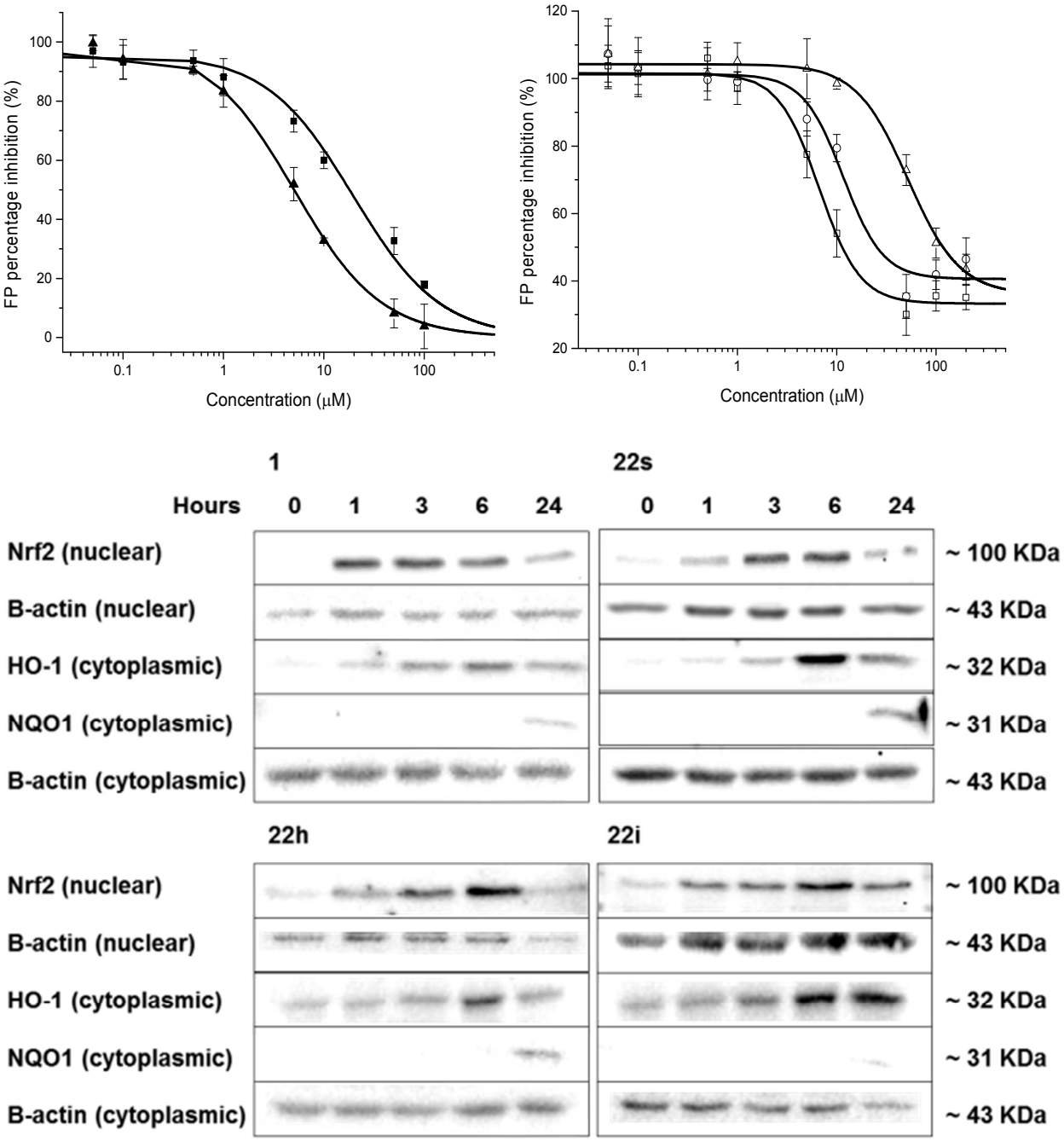

Figure 3. Dose response curves (top) for the fluorescence polarization assays of **3** (▲) and **5** (■) and **22h** (○), **22i** (Δ) and **22s** (□). Western Blot analysis (bottom) demonstrating upregulation of Nrf2 and its downstream targets HO-1 and NQO1 in Hepa1c1c7 cells after exposure to 10 μM concentrations of **1**, **22h**, **22i** and **22s** over a 24 h period.

EGFP Image	EGFP Lifetime	EGFP Lifetime
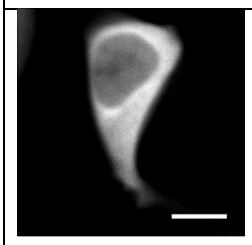 A. Cell 1	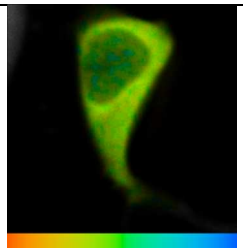 1.9 ns 2.6 ns	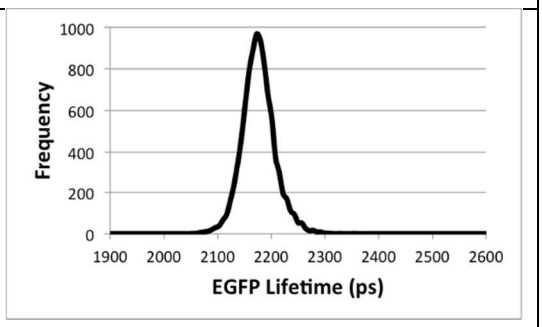
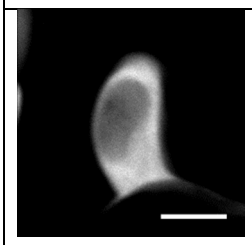 B. Cell 1 + 1 hr	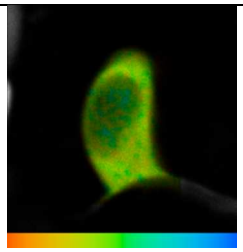 1.9 ns 2.6 ns	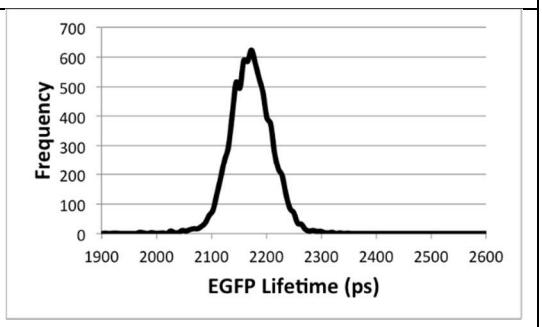
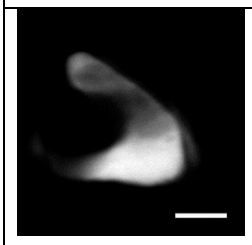 C. Cell 2	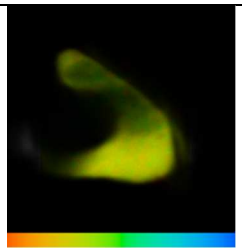 1.9 ns 2.6 ns	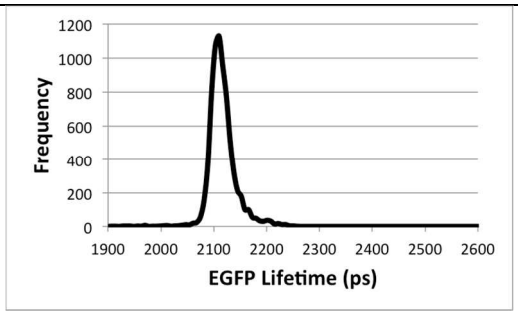
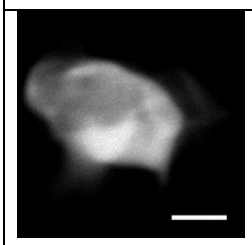 D. Cell 2 + 1 h **22s**	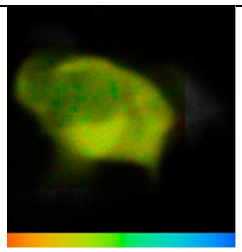 1.9 ns 2.6 ns	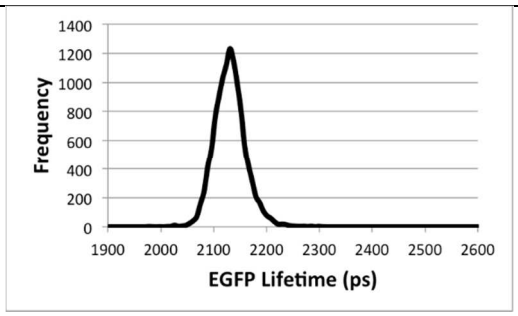

EGFP Image	FRET Efficiency	FRET Efficiency
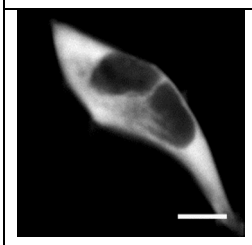 E. Cell 3	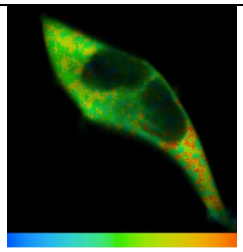 0% 30%	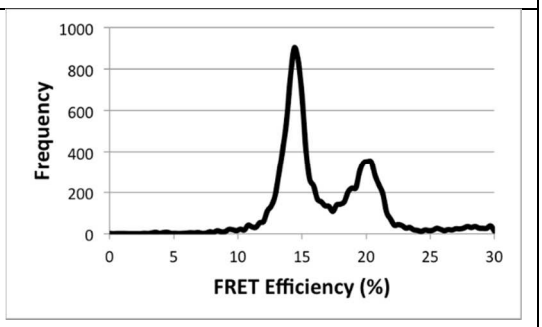
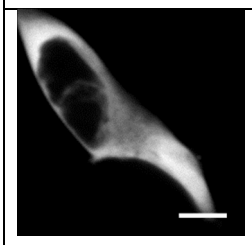 F. Cell 3 + 1 hr **1**	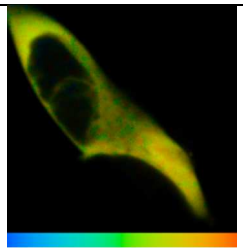 0% 30%	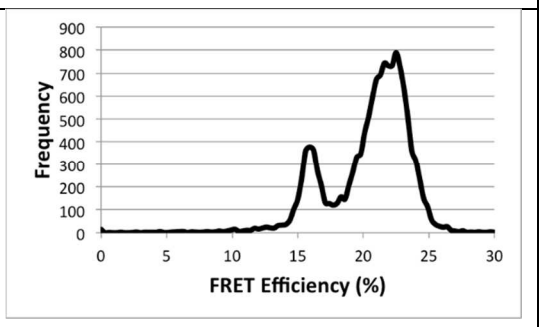
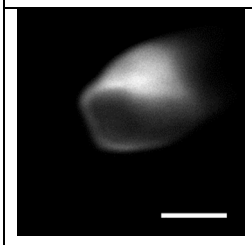 G. Cell 4	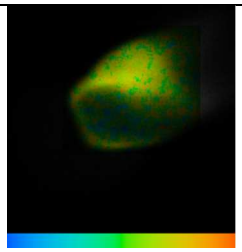 0% 30%	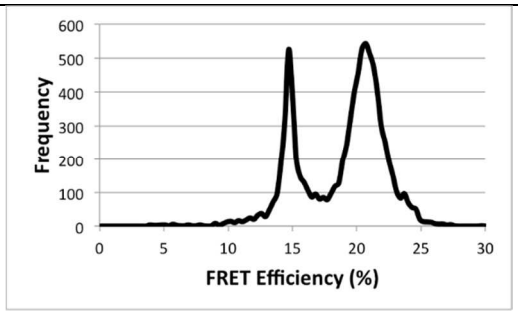
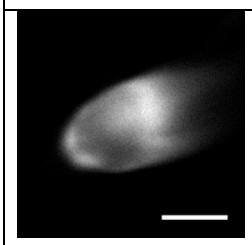 H. Cell 4 + 1 h **22s**	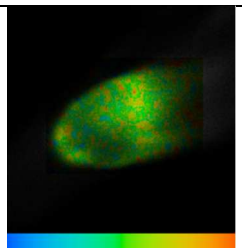 0% 30%	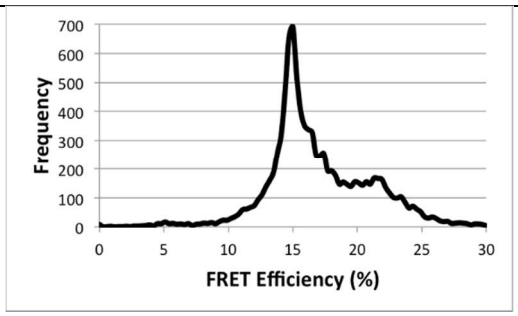

Figure 4. The lifetime and FRET efficiency in the cytoplasm of EGFP-Nrf2 transfected cells imaged before and after treatment with **1** or **22s** for 1 h. HEK293 cells were transfected with EGFP-Nrf2 + Keap1-mCherry, and the lifetime (A-D) and FRET efficiency (E-H) in the cytoplasmic compartment were calculated. A, B show the fluorescence lifetime data from a single cell imaged twice, once at time 0 (A), and once 1 h later (B). C, D show the fluorescence lifetime data from a single cell imaged twice, once at the basal state (C), and once 1 h after treatment with 10 μM **22s** (D). The left column shows the EGFP image from which the lifetime data are derived. The middle column shows a pictorial representation of the EGFP lifetime where the color of the cell corresponds to the lifetime of EGFP, ranging from 1.9 ns to 2.6 ns as indicated on the legend below the image. The right column shows the lifetime data from each pixel of the image plotted on a graph, with lifetime on the x-axis and frequency on the y-axis. E-H show the FRET efficiency data for individual EGFP-Nrf2 + Keap1-mCherry co-transfected cells which were imaged twice, once in the basal state (E, G) and once after 1 h treatment with 5 μM **1** (F) or 10 μM **22s** (H). The left column shows the EGFP image from which the FRET efficiency data are derived. The middle column shows a pictorial representation of the FRET efficiency where the color of the cell corresponds to the FRET efficiency, ranging from 0% to 30% as indicated on the legend below the image. The right column shows the FRET efficiency from each pixel of the image plotted on a graph, with FRET efficiency on the x-axis and frequency on the y-axis. The FRET efficiency graphs (E, F) show that the FRET efficiency distribution is altered by **1**, which leads to an increase in the interaction at 21% FRET efficiency. The FRET efficiency distributions are shown pictorially in the central column of E, F, where an increase in the amount of yellow relative to green can be seen in response to **1** treatment. The FRET efficiency graphs (G, H) show that the FRET efficiency distribution is altered by **22s**,

which leads to an increase in the interaction at 13% FRET efficiency. The FRET efficiency distributions are shown pictorially in the central column of G,H, where an increase in the amount of green relative to yellow can be seen in response to **22s** treatment. White scale bars shown in the figures represent a distance of 10 μm.

SCHEMES

Scheme 1. Synthesis of the 36-member library of 1,4-biaryl-1,2,3-triazole derivatives.

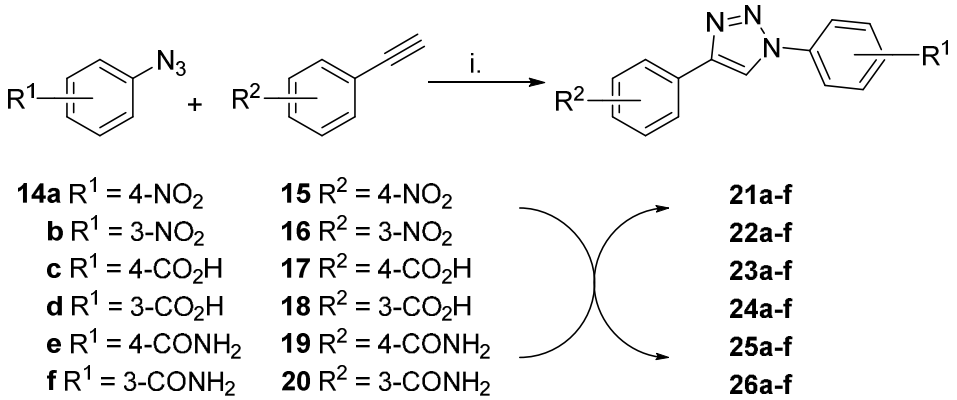

Reagents and conditions: i. $CuSO_4.5H_2O$ (3.3 mol %), ascorbic acid (10.0 mol %), *tert*-butanol/H_2O 1/1, MW, 130 °C, 30 min.

Scheme 2. Synthesis of the refined click library **22g-t**.

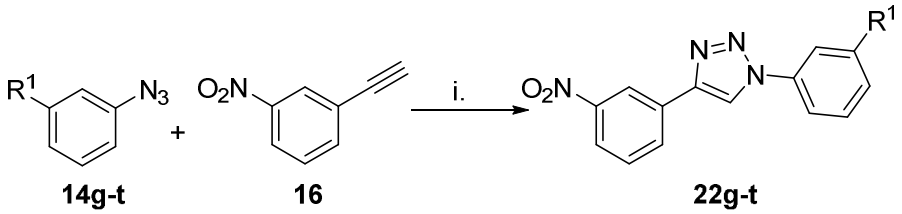

Reagents and conditions: i. see Scheme 1.

Scheme 3. Synthesis of the cyano- and tetrazole-substituted series.

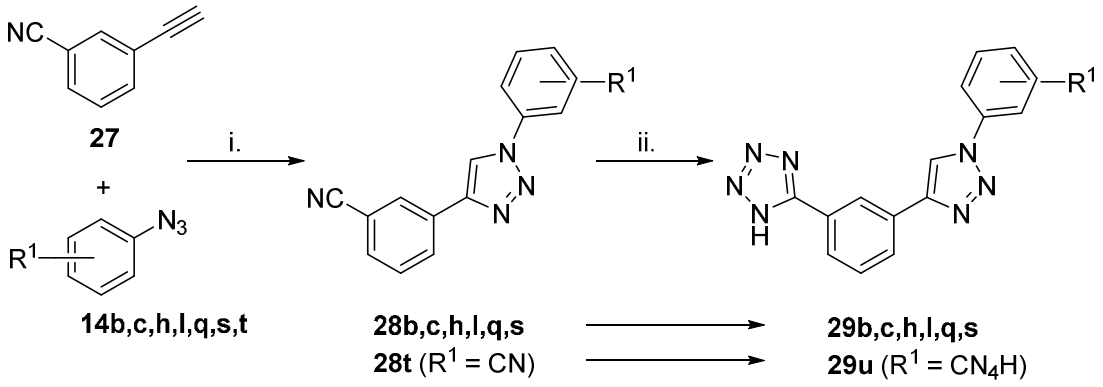

Reagents and conditions: i. see Scheme 1; ii. NH_4Cl (1.25 eq.), NaN_3 (1.25 eq.), LiCl (cat.), DMF, reflux, 24 h.

TABLES.

Table 1. Fixed dose inhibition of the Keap1-Nrf2 interaction (FP) and induction of NQO1 by compounds **21-26**

FP[a]	**21**	**22**	**23**	**24**	**25**	**26**
a	72.6	74.8	83.8	82.3	-[b]	48.0
b	46.5	81.0	87.5	63.8	2.34	32.0
c	81.3	39.4	77.3	92.8	-[b]	70.7
d	61.0	80.1	89.6	82.3	-[b]	78.6
e	46.1	64.5	76.5	87.6	-[b]	-[b]
f	62.2	65.3	15.4	96.3	43.7	53.3

NQO1[c]	**21**	**22**	**23**	**24**	**25**	**26**
a	1.00	3.38	0.89	1.14	1.02	1.05
b	1.81	2.30	1.06	0.85	1.33	2.06
c	0.99	-[d]	0.90	0.78	0.79	0.81
d	0.66	0.83	0.47	0.86	0.79	0.71
e	1.07	2.08	0.86	0.91	0.98	0.72
f	0.98	2.09	0.95	1.07	1.02	1.02

Notes: a. Percentage inhibition at 100 μM; b. Fluorescence interference; c. Fold induction at 10 μM; d. Not determined.

Table 2. Fixed dose inhibition of the Keap1-Nrf2 interaction (FP) and induction of NQO1 by compounds **22b**,**d**,**f-t**

Cpd	R^1	FP[a]	NQO1[b]
22b	NO_2	81.0	2.30
22d	CO_2H	80.1	0.83
22f	$CONH_2$	65.3	2.09
22g	H	66.9	1.95
22h	Me	68.9	2.20
22i	tBu	69.8	1.93
22j	CF_3	66.9	2.54
22k	OMe	68.2	2.56
22l	OEt	69.3	2.48
22m	3,4-OCH_2O	67.2	2.24
22n	SMe	77.7	2.95
22o	NMe_2	65.4	2.91
22p	F	42.6	2.27
22q	Cl	60.4	2.50
22r	Br	68.2	2.94
22s	I	67.2	4.00
22t	CN	36.8	2.33

Notes: a. Percentage inhibition at 100 μM; b. Fold induction at 10 μM.

Table 3. Fixed dose inhibition of the Keap1-Nrf2 interaction (FP) and induction of NQO1 by compounds **28** and **29**

Cpd	R^1	FP[a]	NQO1[b]	Cpd	FP[a]	NQO1[b]
28b	3-NO_2	59.4	2.1	**29b**	71.1	1.75
28c	4-CO_2H	52.8	0.98	**29c**	70.0	1.00
28h	3-Me	49.7	1.69	**29h**	30.4	0.88
28l	3-OEt	24.5	1.30	**29l**	39.6	1.31
28q	3-Cl	19.9	2.39	**29p**	40.7	1.24
28s	3-I	21.9	1.53	**29s**	51.5	1.03
28t	3-CN	58.8	1.92	**29u**[c]	13.7	0.84

Notes: a. Percentage inhibition at 100 μM; b. Fold induction at 10 μM; c. R1 = CN_4H.

Table 4. EC_{50} values determined by FP assay and CD values from the NQO1 induction assay for selected compounds.

Compound	R^1	FP EC_{50} (μM)	NQO1 CD (μM)
22b	3-NO_2	11.5 (± 1.4)	-
22d	3-CO_2H	5.0 (± 1.9)	>10
22g	H	20.6 (± 5.6)	>10
22h	3-Me	10.0 (± 2.7)	1.3
22i	3-tBu	37.8 (± 7.1)	>10
22j	3-CF_3	22.6 (± 6.4)	-
22k	3-OMe	15 (± 5.8)	4.7
22l	3-OEt	11.3 (± 3.3)	-

22m	3,4-OCH_2O	15 (± 3.4)	-
22n	3-SMe	38.5 (± 9.5)	-
22o	3-$N[Me]_2$	12.7 (± 3.1)	2.0
22q	3-Cl	8.8 (± 1.7)	0.7
22r	3-Br	24.5 (± 7.1)	1.2
22s	3-I	7.1 (± 0.7)	0.6
1	-	-	0.3
2	-	-	10.2

ASSOCIATED CONTENT

Supporting Information. Detailed chemical synthesis and experimental procedures for molecular modeling, fluorescence polarization assays, NQO1 assays and Western blot experiments. This material is available free of charge via the Internet at http://pubs.acs.org.

AUTHOR INFORMATION

Corresponding Author

*UCL School of Pharmacy, University College London, London WC1N 1AX. Email: g.wells@ucl.ac.uk, Tel: +44 (0)20 7753 5935, Fax: +44 (0)20 7753 5964.

Present Addresses

† Ecole Normale Supérieure- PSL research University, Sorbonne Universités - UPMC Univ Paris 06, CNRS - UMR7203, Laboratoire des Biomolécules, 24 rue Lhomond, 75005 Paris, France

††Department of Medical Biochemistry, Tohoku University School of Medicine, 2-1 Seiryo-machi, Aoba-ku, Sendai 980-8575, Japan.

Author Contributions

All authors have given approval to the final version of the manuscript.

Funding Sources

The authors acknowledge Cancer Research UK (C9344/A10268) (H.B., A.F., M.S., G.W.) and (C20953/A10270) (A.D-K), the MRC (L.B. and A.D-K), the BBSRC (BB/L01923X/1) (A.D-K and G.W) and the School of Pharmacy (G.W.) for financial support.

ACKNOWLEDGMENT

We thank Dr Tadayuki Tsujita and Prof. John Hayes (University of Dundee) for providing the purified Keap1 Kelch domain protein.

ABBREVIATIONS

FP, fluorescence polarization; GI, growth inhibition.

REFERENCES

1. Kensler, T. W.; Wakabayashi, N.; Biswal, S. Cell survival responses to environmental stresses via the Keap1-Nrf2-ARE pathway. *Annu Rev Pharmacol Toxicol* **2007,** 47, 89-116.

2. Hayes, J. D.; McMahon, M.; Chowdhry, S.; Dinkova-Kostova, A. T. Cancer chemoprevention mechanisms mediated through the Keap1-Nrf2 pathway. *Antioxid Redox Signal* **2010,** 13, 1713-1748.

3. Cheng, X.; Siow, R. C.; Mann, G. E. Impaired redox signaling and antioxidant gene expression in endothelial cells in diabetes: a role for mitochondria and the nuclear factor-E2-related factor 2-Kelch-like ECH-associated protein 1 defense pathway. *Antioxid Redox Signal* **2011,** 14, 469-487.

4. Hong, F.; Sekhar, K. R.; Freeman, M. L.; Liebler, D. C. Specific patterns of electrophile adduction trigger Keap1 ubiquitination and Nrf2 activation. *J Biol Chem* **2005,** 280, 31768-31775.

5. Kobayashi, M.; Yamamoto, M. Nrf2-Keap1 regulation of cellular defense mechanisms against electrophiles and reactive oxygen species. *Adv Enzyme Regul* **2006,** 46, 113-140.

6. Itoh, K.; Wakabayashi, N.; Katoh, Y.; Ishii, T.; Igarashi, K.; Engel, J. D.; Yamamoto, M. Keap1 represses nuclear activation of antioxidant responsive elements by Nrf2 through binding to the amino-terminal Neh2 domain. *Gene Dev* **1999,** 13, 76-86.

7. Kobayashi, A.; Kang, M. I.; Okawa, H.; Ohtsuji, M.; Zenke, Y.; Chiba, T.; Igarashi, K.; Yamamoto, M. Oxidative stress sensor Keap1 functions as an adaptor for Cul3-based E3 ligase to regulate proteasomal degradation of Nrf2. *Mol Cell Biol* **2004,** 24, 7130-9.

8. Zhang, D. D.; Hannink, M. Distinct cysteine residues in Keap1 are required for Keap1-dependent ubiquitination of Nrf2 and for stabilization of Nrf2 by chemopreventive agents and oxidative stress. *Mol Cell Biol* **2003,** 23, 8137-8151.

9. Furukawa, M.; Xiong, Y. BTB protein Keap1 targets antioxidant transcription factor Nrf2 for ubiquitination by the Cullin 3-Roc1 ligase. *Mol Cell Biol* **2005,** 25, 162-71.

10. Tong, K. I.; Katoh, Y.; Kusunoki, H.; Itoh, K.; Tanaka, T.; Yamamoto, M. Keap1 recruits Neh2 through binding to ETGE and DLG motifs: characterization of the two-site molecular recognition model. *Mol Cell Biol* **2006,** 26, 2887-900.

11. Baird, L.; Lleres, D.; Swift, S.; Dinkova-Kostova, A. T. Regulatory flexibility in the Nrf2-mediated stress response is conferred by conformational cycling of the Keap1-Nrf2 protein complex. *Proc Natl Acad Sci U S A* **2013,** 110, 15259-15264.

12. Tong, K. I.; Padmanabhan, B.; Kobayashi, A.; Shang, C.; Hirotsu, Y.; Yokoyama, S.; Yamamoto, M. Different electrostatic potentials define ETGE and DLG motifs as hinge and latch in oxidative stress response. *Mol Cell Biol* **2007,** 27, 7511-21.

13. Padmanabhan, B.; Tong, K. I.; Ohta, T.; Nakamura, Y.; Scharlock, M.; Ohtsuji, M.; Kang, M. I.; Kobayashi, A.; Yokoyama, S.; Yamamoto, M. Structural basis for defects of Keap1 activity provoked by its point mutations in lung cancer. *Mol Cell* **2006,** 21, 689-700.

14. Lo, S. C.; Li, X.; Henzl, M. T.; Beamer, L. J.; Hannink, M. Structure of the Keap1:Nrf2 interface provides mechanistic insight into Nrf2 signaling. *EMBO J* **2006,** 25, 3605-17.

15. McMahon, M.; Thomas, N.; Itoh, K.; Yamamoto, M.; Hayes, J. D. Dimerization of substrate adaptors can facilitate cullin-mediated ubiquitylation of proteins by a "tethering" mechanism: a two-site interaction model for the Nrf2-Keap1 complex. *J Biol Chem* **2006,** 281, 24756-68.

16. Kobayashi, M.; Li, L.; Iwamoto, N.; Nakajima-Takagi, Y.; Kaneko, H.; Nakayama, Y.; Eguchi, M.; Wada, Y.; Kumagai, Y.; Yamamoto, M. The antioxidant defense system Keap1-Nrf2 comprises a multiple sensing mechanism for responding to a wide range of chemical compounds. *Mol Cell Biol* **2009,** 29, 493-502.

17. Baird, L.; Dinkova-Kostova, A. T. The cytoprotective role of the Keap1-Nrf2 pathway. *Arch Toxicol* **2011,** 85, 241-272.

18. Magesh, S.; Chen, Y.; Hu, L. Small molecule modulators of Keap1-Nrf2-ARE pathway as potential preventive and therapeutic agents. *Med Res Rev* **2012,** 32, 687-726.

19. Kensler, T. W.; Egner, P. A.; Agyeman, A. S.; Visvanathan, K.; Groopman, J. D.; Chen, J. G.; Chen, T. Y.; Fahey, J. W.; Talalay, P. Keap1-nrf2 signaling: a target for cancer prevention by sulforaphane. *Top Curr Chem* **2013,** 329, 163-177.

20. Guerrero-Beltran, C. E.; Calderon-Oliver, M.; Pedraza-Chaverri, J.; Chirino, Y. I. Protective effect of sulforaphane against oxidative stress: recent advances. *Exp Toxicol Pathol* **2012,** 64, 503-508.

21. Dinkova-Kostova, A. T. Chemoprotection against cancer by isothiocyanates: a focus on the animal models and the protective mechanisms. *Top Curr Chem* **2013,** 329, 179-201.

22. Kensler, T. W.; Chen, J. G.; Egner, P. A.; Fahey, J. W.; Jacobson, L. P.; Stephenson, K. K.; Ye, L.; Coady, J. L.; Wang, J. B.; Wu, Y.; Sun, Y.; Zhang, Q. N.; Zhang, B. C.; Zhu, Y. R.; Qian, G. S.; Carmella, S. G.; Hecht, S. S.; Benning, L.; Gange, S. J.; Groopman, J. D.; Talalay,

P. Effects of glucosinolate-rich broccoli sprouts on urinary levels of aflatoxin-DNA adducts and phenanthrene tetraols in a randomized clinical trial in He Zuo township, Qidong, People's Republic of China. *Cancer Epidemiol Biomarkers Prev* **2005,** 14, 2605-2613.

23. Egner, P. A.; Chen, J. G.; Zarth, A. T.; Ng, D. K.; Wang, J. B.; Kensler, K. H.; Jacobson, L. P.; Munoz, A.; Johnson, J. L.; Groopman, J. D.; Fahey, J. W.; Talalay, P.; Zhu, J.; Chen, T. Y.; Qian, G. S.; Carmella, S. G.; Hecht, S. S.; Kensler, T. W. Rapid and sustainable detoxication of airborne pollutants by broccoli sprout beverage: results of a randomized clinical trial in China. *Cancer Prev Res* **2014,** 7, 813-823.

24. Singh, K.; Connors, S. L.; Macklin, E. A.; Smith, K. D.; Fahey, J. W.; Talalay, P.; Zimmerman, A. W. Sulforaphane treatment of autism spectrum disorder (ASD). *Proc Natl Acad Sci U S A* **2014,** 111, 15550-15555.

25. Hancock, R.; Bertrand, H. C.; Tsujita, T.; Naz, S.; El-Bakry, A.; Laoruchupong, J.; Hayes, J. D.; Wells, G. Peptide inhibitors of the Keap1-Nrf2 protein-protein interaction. *Free Radic Biol Med* **2012,** 52, 444-451.

26. Hancock, R.; Schaap, M.; Pfister, H.; Wells, G. Peptide inhibitors of the Keap1-Nrf2 protein-protein interaction with improved binding and cellular activity. *Org Biomol Chem* **2013,** 11, 3553-3557.

27. Steel, R.; Cowan, J.; Payerne, E.; O'Connell, M. A.; Searcey, M. Anti-inflammatory effect of a cell-penetrating peptide targeting the Nrf2/Keap1 interaction. *ACS Med Chem Lett* **2012,** 3, 407-410.

28. Chen, Y.; Inoyama, D.; Kong, A. N.; Beamer, L. J.; Hu, L. Kinetic analyses of Keap1-Nrf2 interaction and determination of the minimal Nrf2 peptide sequence required for Keap1 binding using surface plasmon resonance. *Chem Biol Drug Des* **2011,** 78, 1014-1021.

29. Inoyama, D.; Chen, Y.; Huang, X.; Beamer, L. J.; Kong, A. N.; Hu, L. Optimization of fluorescently labeled Nrf2 peptide probes and the development of a fluorescence polarization assay for the discovery of inhibitors of Keap1-Nrf2 interaction. *J Biomol Screen* **2011,** 17, 435-447.

30. Sun, H.-P.; Jiang, Z.-Y.; Zhang, M.-Y.; Lu, M.-C.; Yang, T.-T.; Pan, Y.; Huang, H.-Z.; Zhang, X.-J.; You, Q.-d. Novel protein–protein interaction inhibitor of Nrf2–Keap1 discovered by structure-based virtual screening. *MedChemComm* **2014,** 5, 93-98.

31. Zhuang, C.; Narayanapillai, S.; Zhang, W.; Sham, Y. Y.; Xing, C. Rapid identification of Keap1-Nrf2 small-molecule inhibitors through structure-based virtual screening and hit-based substructure search. *J Med Chem* **2014,** 57, 1121-1126.

32. Hu, L.; Magesh, S.; Chen, L.; Wang, L.; Lewis, T. A.; Chen, Y.; Khodier, C.; Inoyama, D.; Beamer, L. J.; Emge, T. J.; Shen, J.; Kerrigan, J. E.; Kong, A. N.; Dandapani, S.; Palmer, M.; Schreiber, S. L.; Munoz, B. Discovery of a small-molecule inhibitor and cellular probe of Keap1-Nrf2 protein-protein interaction. *Bioorg Med Chem Lett* **2013,** 23, 3039-3043.

33. Marcotte, D.; Zeng, W.; Hus, J. C.; McKenzie, A.; Hession, C.; Jin, P.; Bergeron, C.; Lugovskoy, A.; Enyedy, I.; Cuervo, H.; Wang, D.; Atmanene, C.; Roecklin, D.; Vecchi, M.; Vivat, V.; Kraemer, J.; Winkler, D.; Hong, V.; Chao, J.; Lukashev, M.; Silvian, L. Small molecules inhibit the interaction of Nrf2 and the Keap1 Kelch domain through a non-covalent mechanism. *Bioorg Med Chem* **2013,** 21, 4011-4019.

34. Jnoff, E.; Albrecht, C.; Barker, J. J.; Barker, O.; Beaumont, E.; Bromidge, S.; Brookfield, F.; Brooks, M.; Bubert, C.; Ceska, T.; Corden, V.; Dawson, G.; Duclos, S.; Fryatt, T.; Genicot, C.; Jigorel, E.; Kwong, J.; Maghames, R.; Mushi, I.; Pike, R.; Sands, Z. A.; Smith, M. A.;

Stimson, C. C.; Courade, J. P. Binding mode and structure-activity relationships around direct inhibitors of the Nrf2-Keap1 complex. *ChemMedChem* **2014,** 9, 699-705.

35. Jiang, Z. Y.; Lu, M. C.; Xu, L. L.; Yang, T. T.; Xi, M. Y.; Xu, X. L.; Guo, X. K.; Zhang, X. J.; You, Q. D.; Sun, H. P. Discovery of potent Keap1-Nrf2 protein-protein interaction inhibitor based on molecular binding determinants analysis. *J Med Chem* **2014,** 57, 2736-2745.

36. Li, X.; Zhang, D.; Hannink, M.; Beamer, L. J. Crystal structure of the Kelch domain of human Keap1. *J Biol Chem* **2004,** 279, 54750-54758.

37. Dinkova-Kostova, A. T.; Fahey, J. W.; Talalay, P. Chemical Structures of Inducers of Nicotinamide Quinone Oxidoreductase 1 (NQO1). *Method Enzymol* **2004,** 382, 423-448.

38. Fahey, J. W.; Dinkova-Kostova, A. T.; Stephenson, K. K.; Talalay, P. The "Prochaska" microtiter plate bioassay for inducers of NQO1. *Method Enzymol* **2004,** 382, 243-258.

39. East, D. A.; Fagiani, F.; Crosby, J.; Georgakopoulos, N. D.; Bertrand, H.; Schaap, M.; Fowkes, A.; Wells, G.; Campanella, M. PMI: A ΔΨm independent pharmacological regulator of mitophagy. *Chem Biol* **2014,** 21, 1585-1596.

40. Irwin, J. J.; Sterling, T.; Mysinger, M. M.; Bolstad, E. S.; Coleman, R. G. ZINC: a free tool to discover chemistry for biology. *J Chem Inf Model* **2012,** 52, 1757-1768.

41. Morris, G. M.; Huey, R.; Lindstrom, W.; Sanner, M. F.; Belew, R. K.; Goodsell, D. S.; Olson, A. J. AutoDock4 and AutoDockTools4: automated docking with selective receptor flexibility. *J Comput Chem* **2009,** 30, 2785-2791.

42. Brozell, S. R.; Mukherjee, S.; Balius, T. E.; Roe, D. R.; Case, D. A.; Rizzo, R. C. Evaluation of DOCK 6 as a pose generation and database enrichment tool. *J Comput Aided Mol Des* **2012,** 26, 749-773.

43. Baell, J. B.; Holloway, G. A. New substructure filters for removal of pan assay interference compounds (PAINS) from screening libraries and for their exclusion in bioassays. *J Med Chem* **2010,** 53, 2719-2740.

44. Tipparaju, S. K.; Muench, S. P.; Mui, E. J.; Ruzheinikov, S. N.; Lu, J. Z.; Hutson, S. L.; Kirisits, M. J.; Prigge, S. T.; Roberts, C. W.; Henriquez, F. L.; Kozikowski, A. P.; Rice, D. W.; McLeod, R. L. Identification and development of novel inhibitors of Toxoplasma gondii enoyl reductase. *J Med Chem* **2010,** 53, 6287-6300.

45. Perez-Medrano, A.; Nelson, D. W.; Carroll, W. A.; Kort, M. E.; Gregg, R. J.; Voight, E. A.; Jarvis, M. F.; Kowaluk, E. A. The use of selective P2X7 receptor antagonists. WO2006086229 A1, 2006, 2006.

46. Cornblatt, B. S.; Ye, L.; Dinkova-Kostova, A. T.; Erb, M.; Fahey, J. W.; Singh, N. K.; Chen, M. S.; Stierer, T.; Garrett-Mayer, E.; Argani, P.; Davidson, N. E.; Talalay, P.; Kensler, T. W.; Visvanathan, K. Preclinical and clinical evaluation of sulforaphane for chemoprevention in the breast. *Carcinogenesis* **2007,** 28, 1485-1490.

47. Baird, L.; Swift, S.; Lleres, D.; Dinkova-Kostova, A. T. Monitoring Keap1-Nrf2 interactions in single live cells. *Biotechnol Adv* **2014,** 32, 1133-1144.

Table of Contents Graphic

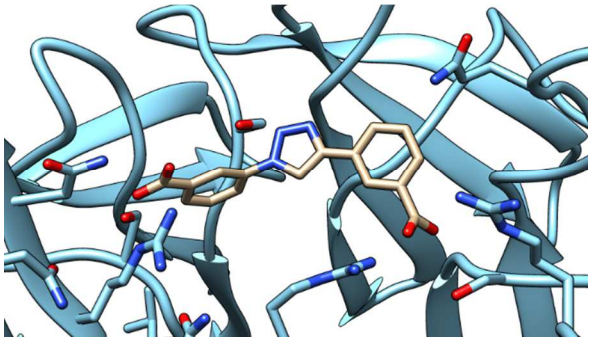

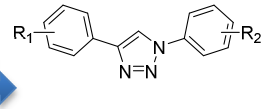

R^1 = 3-NO_2; R^2 = 3-Me, Cl, or I:
EC_{50} = 7.1 - 10.0 μM, CD (NQO1) = 0.6 - 1.3 μM